ISSN: 2414-1895 DOI: 10.6919/ICJE.202105_7(5).0022

Study on Characteristics of Liquid Flow Field in A^2/O Reactor Based on Laser Velocimetry

Jianjun Zhang, Tao Zeng

Sichuan University of Science & Engineering, Yibin 644000, China.

Abstract

In order to solve the problems of low accuracy and single measuring position in the current method for measuring the flow field characteristics of A^2/O reactor, a laser method for measuring the flow field characteristics of liquid phase in A^2/O reactor was proposed. The system of laser and CCD camera was used to capture the particle displacement in A^2/O reactor at different time periods. The camera divides the captured particle image into several zones, each of which generates the corresponding particle displacement vector. Then, the sub-pixel interpolation method is used to measure the particle velocity in A^2/O reactor to improve the measurement accuracy. The experimental results show that the proposed method can accurately measure the flow characteristics of the internal flow field in A^2/O reactor, and has the advantages of wide detection position, transient and high accuracy.

Keywords

Laser Velocimetry; A^2/O Reactor; Liquid State; Flow Field Characteristics.

1. Introduction

A^2/O process is commonly used in urban sewage treatment plants [1], and has been widely used in various sewage treatment occasions [2-3], and has good treatment effect of ammonia nitrogen, BOD and COD [4]. In order to improve the treatment effect of A^2/O reactor, it is necessary to optimize its structure, and the flow field characteristics inside the reactor is very important for the design of the reactor. Therefore, it is of great significance to study the flow field characteristics of the fluid in the reactor for enhancing the wastewater treatment effect of the reactor. At present, the research on the internal flow field of A^2/O reactor mainly adopts the method of software simulation, which is not intuitive and accurate [5-7].

Zhang Zhi [8] used FLUENT software as a tool to simulate the flow field in anoxic zone of A^2/O oxidation ditch of Chongqing wellhead sewage treatment plant by using three-dimensional RNG k-ε turbulence mathematical model. Through the simulation results after optimization, it can be seen that the flow field in the anoxic zone is more evenly distributed under the same power density, and the flow velocity is increased from 0.131m/s to 0.204 m/s, which reduces the energy loss. The flow rate at the bottom was also increased from 0.140 m/s to 0.226 m/s, which effectively prevented or reduced the sludge deposition in the ditch. Huang Wei [9] studied the vertical and horizontal velocity distribution and the vertical average velocity transverse distribution on the flow measurement section by selecting the flow measurement data of two hydrological stations, Jinghe and Sheyang sluices. The results show that: for the straight river, the velocity distribution at the vertical point basically conforms to the theoretical velocity distribution; for the flow measuring section affected by the tide, the relative velocity fluctuation and homogenization have great influence, so it is difficult to find the velocity distribution law. Liu Zijun [10] theoretically analyzed the interference fringe spacing and gradient distribution in the volume measured by laser Doppler velocimeter. The waist radii of green light and purple light are 114 μ m and 83 μ m respectively, and the spatial position of the waist is

ISSN: 2414-1895 DOI: 10.6919/ICJE.202105_7(5).0022

determined. Compared with the results of green and purple interference fringes measured by turntable, the theoretical analysis and measurement results of interference fringes distribution are verified. The maximum relative errors are 0.87% and 0.78% respectively. There are some errors in the measurement results obtained by the above three methods, and references [9] and [10] can not realize the measurement of the whole flow field.

In conclusion, a method of measuring the characteristics of liquid flow field in A^2/O reactor by laser velocimetry is proposed.

2. Principle

Laser particle image velocimetry is a non-invasive, full flow optical technology used to obtain the velocity information of particles suspended in the fluid [11]. It is based on the measurement of the particle displacement in a known time interval. Therefore, the particle velocity can be calculated by the following formula:

$$v = \frac{s}{t}$$

Where V is the velocity of the particle, s is the displacement of the particle in a certain period of time, and t is the time.

As shown in Figure 1, the measurement system is mainly composed of laser and camera. The particle displacement is detected in a given area of the flow field to be measured. The flow field area is illuminated by laser sheet light, which usually produces stroboscopic effect by pulse, and freezes the movement of tracer particles with the passage of time. The position of the illuminated tracer particles is captured by CCD or CMOS camera. The angle between the camera and the sheet light is right angle. In each camera frame, the tracer particles will appear in the form of bright spots on the dark background. The correct choice of tracer particle type depends on the properties of the flow studied. In addition, the light source and the camera are synchronized, so the tracer particles illuminated at the time of the light pulse number 1 are captured by the camera frame 1, while the particles from the light pulse number 2 are captured by the camera frame 2.

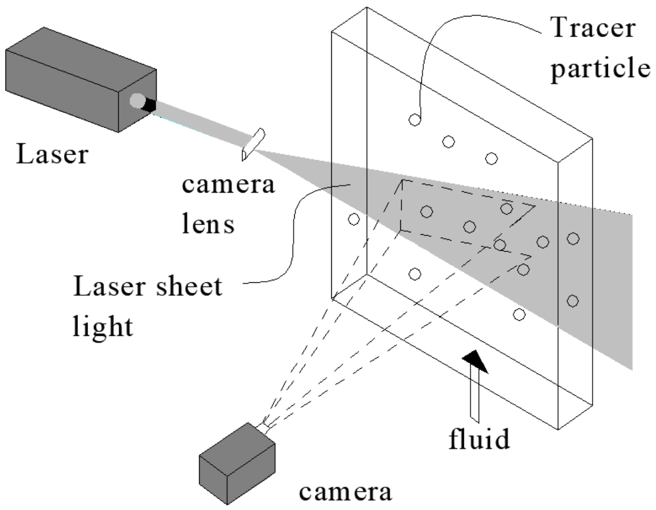

Figure 1. Schematic diagram of measurement system

The image captured by the camera gets the particle velocity through the process shown in Figure 2. The camera divides the image into (M×N pixels) query areas, each of which is correlated to produce an average particle displacement vector. Doing this for all the query areas produces a vector graph. The displacement of the camera (in pixels) is converted to the physical size (in nm), and then the particle velocity is obtained according to the particle velocity formula [12].

ISSN: 2414-1895
DOI: 10.6919/ICJE.202105_7(5).0022

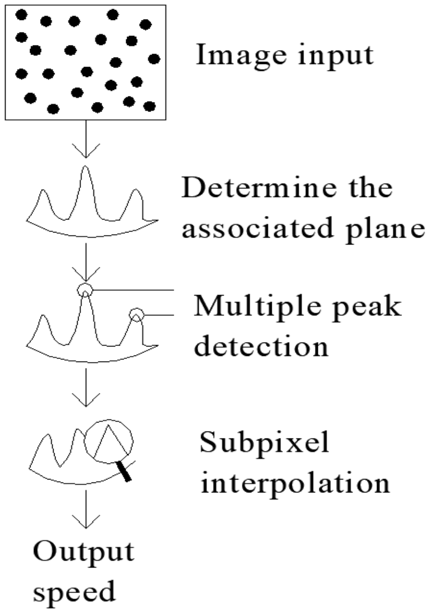

Figure 2. Post processing flow of vector graph

The image mapping is processed by FFT to determine the correlation plane, and then multi peak detection is carried out: scan the correlation plane: (I) autocorrelation peak and two peaks are detected in autocorrelation; (II) cross correlation peak and two peaks are detected in cross correlation. For each peak detected in the correlation plane, two-dimensional curve fitting is used to estimate the width, height and position of the peak. In general, Gaussian interpolation method [13-14] is adopted, assuming that the peak value is a symmetric Gaussian curve without baseline offset, and the interpolation function is as follows:

$$f(x,y) = h * \exp\left[-4 \cdot \frac{(x-x_0)^2 + (y-y_0)^2}{w^2}\right]$$

Where (x_0, y_0) is the position of the peak, (h, w) is the height and width of the peak.
Width W is the full width of e^{-1}, that is at 37% of the peak value. The standard deviation σ (representing the half width of $e^{-\frac{1}{2}}$ level, which is at 61% of the peak value) is used as the width parameter of Gaussian curve.

$$f(x) = h \cdot \exp(-\frac{x^2}{2 \cdot \sigma^2})$$

$$w = 2 \cdot \sqrt{2} \cdot \sigma$$

$$f(x,y) = h \cdot \exp\left[-4 \cdot \frac{(x-x_0)^2}{w^2}\right] \cdot exp\left[-4 \cdot \frac{(y-y_0)^2}{w^2}\right]$$

$$\frac{\partial}{\partial x} f(x,y) = h \cdot \frac{-8}{w^2}(x-x_0) \cdot f(x,y)$$

$$\frac{\partial}{\partial y} f(x,y) = h \cdot \frac{-8}{w^2}(y-y_0) \cdot f(x,y)$$

Through the above steps, the velocity in the flow field can be measured, and on this basis, the characteristics of velocity field, vorticity field and streamline can be measured.

3. Experiment and result analysis

The flow chart of A^2/O reactor test system is shown in Figure 3. The test system is mainly composed of water inlet and outlet system, A^2/O reactor, laser system, CCD camera system and computer.

ISSN: 2414-1895 DOI: 10.6919/ICJE.202105_7(5).0022

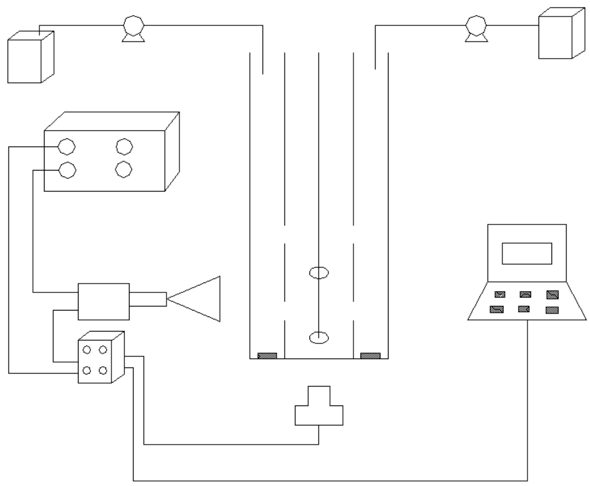

Figure 3. Flow chart of fluidized bed test system

The reactor is composed of aerobic anoxic aerobic three cells in series. The bottom of the left and right cells are equipped with aeration plates, the middle cell is equipped with stirring device, and the left and right cells are separated from the middle cell by guide plates. There are two circulation openings on the guide plate to increase the material exchange between the left and right cells and the middle cell. The center of the lower circulation opening is 700mm from the top, and its size is 100mm×33mm (length×width). The structural size of the whole model is 0.36m×0.13m×0.8m, and the total volume is 37.4L. The stirring shaft of the stirring system is located in the center of the middle cell, and two blades are hung on the shaft, with a blade span of 50mm and an aperture of 8mm. Rhodamine B fluorescent polymer particles were selected as tracer in the experiment, and the particle size was 20~50 μm; the tracer suspension was red, and its density was about equal to the density of deionized water. Distilled water was used in the experiment, and the density and viscosity of sewage were close to that of distilled water.

The laser light source enters from the left side of the reactor, as shown in Figure 1. The CCD camera is placed on the front of the reactor, perpendicular to the direction of the laser light source. The total volume of the reactor is 37.4 L and the effective water depth is 0.6 m. In order to obtain better shooting effect, the measurement area (360mm×270mm) is near the position of the lower circulation port, as shown in Figure 4, and the shooting section is 30mm away from the blade of the mixing shaft.

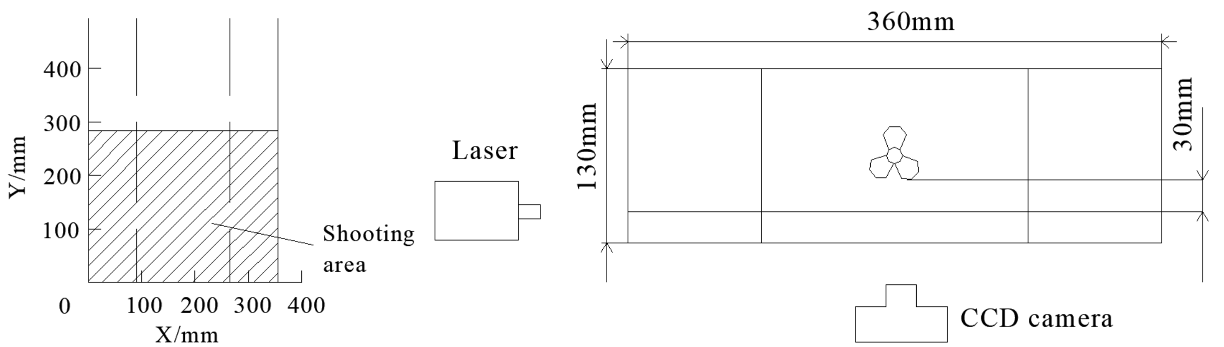

(a) Shooting area map (b) Laser section

Figure 4. Shooting position

Fig. 5 is the curve of the average radial and axial velocity and vorticity of the liquid in the lower part of the reactor with different stirring speeds; FIG. 6 is the streamline and vorticity diagram under different stirring speeds.

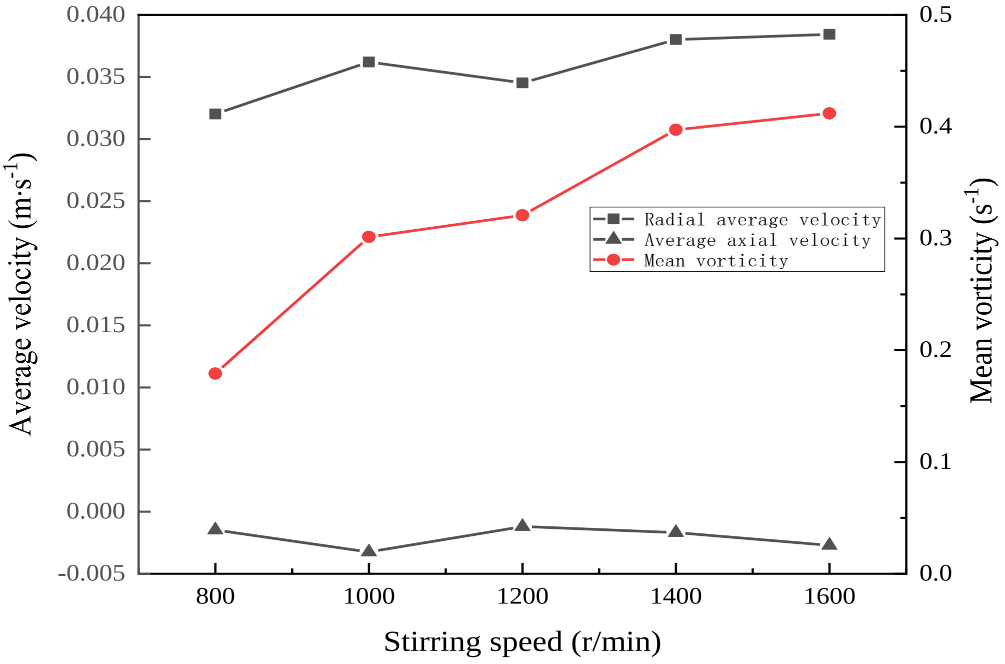

Figure 5. The curves of the radial and axial average velocity and vorticity of liquid in the lower region of the reactor with the change of stirring speed

It can be seen from Figure 5 that: the axial average velocity of liquid changes little; the radial average velocity first increases, then decreases and then increases with the increase of stirring speed; the average vorticity of liquid gradually increases with the increase of stirring speed; when the stirring speed is 1600 r/min, the radial average velocity and average vorticity reach the peak values of 0.0384 m/s and 0.4119 s^{-1} respectively. It shows that the liquid phase mixing degree is good, and the good liquid phase flow state is helpful to promote the reaction between microorganism and wastewater, and improve the treatment efficiency of the reactor.

It can be seen from the analysis in Fig. 5 that the average radial velocity and vorticity of liquid in the lower part of the reactor increase with the change of stirring speed. The reason is analyzed, when the stirring speed is high, the fluid from the upper annular outlet flows downward under the action of stirring, the larger rotation speed of the stirring shaft enhances the convection between the fluids, and the stronger convection between the fluids increases the radial average velocity; when the stirring speed is small, the influence of the very small rotation speed on the fluid is weak; at the same time, due to the low stirring speed of the particles and fluid at the bottom It is difficult to flow upward, which leads to the decrease of radial flow and velocity.

The flow characteristics in the lower part of the reactor are shown in Fig. 6 (a) - Fig. 4 (e), which shows that the streamline near the stirring shaft is close to the horizontal, vertical and inclined state. With the increase of stirring speed, the area of vorticity distribution is more uniform, and the area of positive vorticity area gradually increases (the vorticity value is positive when the vorticity rotation direction is clockwise, and negative when the vorticity rotation direction is counterclockwise), which indicates that most fluids are rotating clockwise, which is opposite to the rotation direction of the main circulation flow in the flow field, thus enhancing the convection between fluids, and the liquid mixing effect is good. When the stirring speed is 800, 1200 and 1600r / min, a large vortex structure is formed near the top of the section 120mm away from the Y-axis, and the negative vorticity region is concentrated in the vortex structure region. With the increase of stirring speed, the vortex area decreases gradually.

ISSN: 2414-1895 DOI: 10.6919/ICJE.202105_7(5).0022

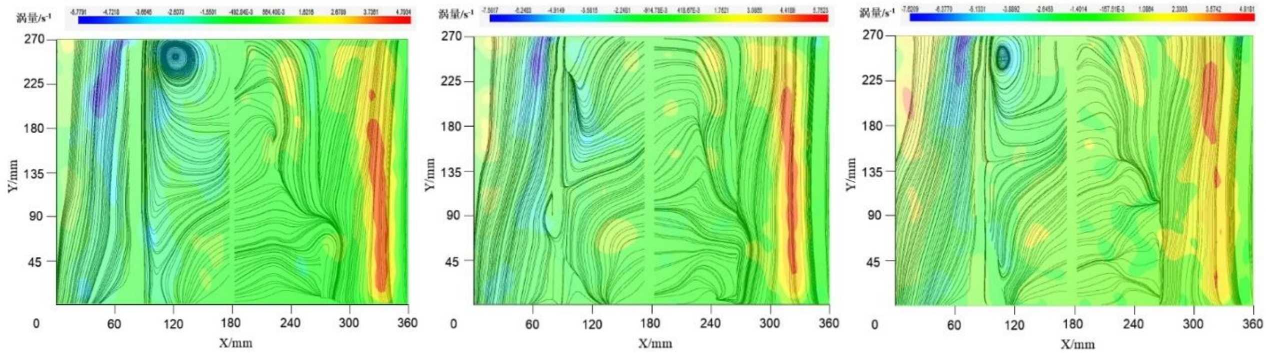

(a) speed 800r/min (b) speed 1000r/min (c) speed 1200r/min

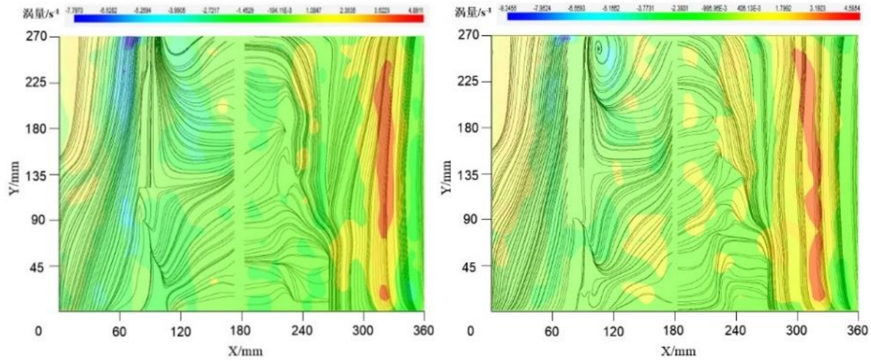

(d) speed 1400r/min (e) speed 1600r/min

Figure 6. Streamline and vorticity in the lower part of a fluidized bed at different stirring speeds

It can be seen from the analysis in Fig. 6 that when the stirring speed is low, the bubbles generated by the aeration in the left cell flow to the middle cell through the circulation port. During the rising process, due to the small pressure, the bubble diameter gradually increases and the buoyancy increases. At the same time, the resistance, lift and additional force generated by the gas-liquid two-phase increase during the rising of bubbles, and the bubbles continue to break and fuse, resulting in the improvement of gas-liquid two-phase mass transfer The liquid phase velocity increases with the increase of temperature. When it reaches the upper part of the cross section, the fluid driven by the stirring shaft collides with the gas-liquid two-phase upward flow, which makes the liquid flow field fluctuate greatly in the upper part of the cross section and forms a vortex structure. When the center distance of the circulation mouth increases, the vortex structure gradually disappears and the liquid flow state is stable.

In conclusion, the stirring speed has a great influence on the flow field characteristics of A^2/O reactor. The experimental results show that when the height of A^2/O reactor is 800 mm, the center distance of circulation ports is 200 mm, and the stirring speed is 1400-1600 r/min, the overall flow field characteristics of A^2/O reactor are ideal. It can be seen from Fig. 5 and Fig. 6 that the method proposed in this paper can accurately measure the flow field characteristics of liquid phase in A^2/O reactor, and the location of measurement is wide, which realizes the measurement of the whole flow field, and provides the basis for the research of A^2/O reactor sewage treatment

4. Conclusion

With the wide application of A^2/O process in wastewater treatment, it is very important to study the flow field characteristics in the reactor. The current flow field measurement methods can not accurately measure the internal velocity of the reactor. The experimental results are as follows:

(1) By analyzing the experimental velocity, the flow field characteristics in A^2/O reactor were measured.

ISSN: 2414-1895 DOI: 10.6919/ICJE.202105_7(5).0022

(2) The accuracy of laser velocimetry in measuring the flow field characteristics in A2 / O reactor is proved by experiments.

(3) The experimental results show that when the height of A^2/O reactor is 800 mm, the center distance of circulation ports is 200 mm, and the stirring speed is 1400-1600 r / min, the overall flow field characteristics of A^2/O reactor are ideal.

Acknowledgments

Supported by The Innovation Fund of Postgraduate, Sichuan University of Science & Engineering (y2019006).

References

[1] Li Yihuan, Zhang Huimin, Wang Yanhong. Application of different water treatment processes in sewage treatment plant [J]. Water treatment technology,2020,46(08):135-140.

[2] Xia Bin, Sheng Xiaolin, Xu Feng. Effect of combined process of A2/O and constructed wetland on rural domestic sewage treatment in Yangtze River delta plain [J/OL]. Journal of Environmental Engineering:1-13[2020-11-08].

[3] Chen Jiangjie, he Leilei, Liu Rui. Effect of A2/O treatment on rural domestic sewage in Yangtze River delta plain [J]. Water supply and drainage in China,2020,36(09):75-82.

[4] Zhang Jiku, sun Mian. Experimental study on treatment of rural domestic sewage by air lift A2/O [J/OL]. Environmental Engineering:1-10[2020-11-08].

[5] Ning Xiaobin, sun Xinming, she yini. Dem-cfd coupling simulation of stirred mill and strength analysis of agitator [J]. Nonferrous Metal Engineering,2016,6(04):63-67+72.

[6] Hong Hao, Chen Xi. Comparative study on structure parameter optimization and Simulation of moving magnet linear motor [J]. Cryogenics and Superconductivity,2020,48(10):55-61.

[7] Li tolei, Wang Junli, Lei Shuai. Numerical simulation method for structural characteristics of twin screw compressor rotor [J]. Mechanical and electrical engineering,2020,37(10):1192-1197+1209.

[8] Zhang Zhi, Chai Hua, Li Bolin. Three dimensional flow field simulation and structure optimization in anoxic zone of A2/O oxidation ditch [J]. Journal of Environmental Engineering,2012,6(01):46-50.

[9] Huang Wei, Tang Yunyi, Zhao Deyou. Study on cross section velocity distribution based on Acoustic Doppler current meter [J]. Water conservancy informatization,2017(04):61-67.

[10] Liu Zijun, Cui Lishui, Xie Dailiang. Theoretical analysis and measurement of interference fringes of laser Doppler velocimeter [J]. China laser,2017,44(08):175-182.

[11] DEEN N G. Two-phase PIV bubbly flows :status and trend[J].Experiments in Fluids,2002,25(1):97-101.

[12] BRAND O, BALTES H. Micro sensor packaging[J].Micro System Technologies,2002,7:205-208.

[13] Chiu Sung Nok, Ling Leevan, McCourt Michael. On variable and random shape Gaussian interpolations [J]. Applied Mathematics and Computation,2019,377.

[14] Yang Rui, Dai Jiacai, Ruan fan. Gaussian interpolation algorithm with correction coefficient for multiphase flow imaging [J]. Innovation and application of science and technology,2014(34):57.